Published as: Cusack, P.B., Healy, M.G., Ryan, P.C., Burke, I.T., O' Donoghue, L.M.T., Ujaczki, E., Courtney, R. 2018. Enhancement of bauxite residue as a low-cost absorbent for phosphorus in aqueous solution, using seawater and gypsum treatments. Journal of Cleaner Production 179: 217 – 224.

Enhancement of bauxite residue as a low-cost adsorbent for phosphorus in aqueous solution, using seawater and gypsum treatments.

Patricia B. Cusack[a,b,c], Mark G. Healy[b*], Paraic C. Ryan[b], Ian T. Burke[d], Lisa M. T. O' Donoghue[e], Éva Ujaczki[c,e,f], Ronan Courtney[a,c]

[a]Department of Biological Sciences, University of Limerick, Castletroy, Co. Limerick, Ireland.

[b]Civil Engineering, National University of Ireland, Galway, Ireland.

[c]The Bernal Institute, University of Limerick, Castletroy, Co. Limerick, Ireland.

[d]School of Earth and Environment, University of Leeds, Leeds LS2 9JT, United Kingdom.

[e]Design and Manufacturing Technology, University of Limerick, Castletroy, Co. Limerick, Ireland.

[f]Department of Applied Biotechnology and Food Science, Faculty of Chemical Technology and Biotechnology, Budapest University of Technology and Economics, Műegyetem rkp. 3, 1111 Budapest, Hungary

*Corresponding Author. Tel: +353 91 495364; fax: +353 91 494507. E-mail address: mark.healy@nuigalway.ie

Highlights

- Separate size fractions of bauxite residue were treated with gypsum and seawater.
- Alkalinity was reduced following treatment with the gypsum and seawater.

- The effect on composition and P adsorption of the treated samples were examined.
- Gypsum was found to be the most successful in enhancing the P adsorption capacity.

Abstract

Bauxite residue (red mud), the by-product produced in the alumina industry, is being produced at an estimated global rate of approximately 150Mt per annum. Due to its highly alkaline nature, many refineries use neutralisation techniques such as mud farming (atmospheric carbonation), direct carbonation using carbon dioxide or reactions with seawater, to treat the bauxite residue and reduce its alkalinity prior to disposal in the BRDA (bauxite residue disposal area). Applying a treatment can render the bauxite residue non-hazardous and may also prepare the bauxite residue for reuse, particularly as an adsorbent. In this study, gypsum and seawater treatments were applied to the various bauxite residue samples obtained and the effects on its mineral, elemental and physiochemical properties were examined, as well as the effect on its phosphorus (P) adsorption capacity. It was found that in addition to reducing the alkalinity of all bauxite residue samples used, the P adsorption capacity was also enhanced following amendment with seawater or gypsum, particularly with gypsum. A positive correlation was detected between P adsorption and both Ca and CaO. A negative correlation was detected between the P adsorption and pH of the media. Fitting the data obtained from a batch adsorption experiment to the Langmuir adsorption isotherm, the maximum adsorption capacity was estimated to range from 0.345 to 2.73 mg P per g bauxite residue, highlighting the re-use potential for bauxite residue as an adsorbent for P.

Keywords: bauxite residue; adsorption; bauxite residue filter; aqueous solution; phosphate removal

1. Introduction

During the extraction of alumina from bauxite ore using the Bayer process, a by-product called bauxite residue (red mud) (Kirwan et al., 2013; Liu et al., 2014) is produced. The global inventory for bauxite residue is approximately 3 billion tonnes, with an estimated annual production rate of 150 million tonnes (Evans, 2016; Mayes et al., 2016). Bauxite residue is highly alkaline (pH >10) (Goloran et al., 2013), with a high salinity and sodicity (Gräfe et al., 2009). Current best practice within this industry includes careful planning and management of highly engineered bauxite residue disposal areas (BRDAs), avoiding contamination of the surrounding environment (Prajapati et al., 2016). In addition, some refineries use neutralisation techniques for the bauxite residue before disposal into the BRDAs (Klauber et al., 2011; IAI, 2015; Evans 2016). These techniques include (1) direct carbonation, whereby the residue slurry is treated with either carbon dioxide, sulfur dioxide gas, or undergoes intensive mud farming using amphirollers (atmospheric carbonation) (Cooling, 2007; Fois et al. 2007; Dilmore et al., 2009; Evans, 2016) (2) addition of spent acids and/or gypsum ($CaSO_4.2H_2O$) (Kirwan et al., 2013), or (3) reaction of residues with seawater (Hanahan et al., 2004; Palmer and Frost, 2009; Couperthwaite et al., 2014).

Bauxite residues typically comprise very fine particles, ranging from 0.01 μm to 200 μm (Pradhan et al., 1996). Depending on the type of bauxite ore used, in some refineries the bauxite residue undergoes a separation technique during processing (Evans, 2016), which allows it to be separated into two main fractions: a fine fraction with a particle size <100 μm and a coarse fraction with a particle size >150 μm (Eastham et al., 2006; Jones et al., 2012). The coarse fraction mainly consists of quartz (SiO_2), whereas the fine fraction is dominated by iron (Fe) oxides (Snars and Gilkes, 2009). The ratio of the fine to coarse fraction produced is dependent on the bauxite ore used and the Bayer process employed (Li, 2001). Refineries

78 which carry out the separation technique, have found use for the coarse fraction to create
79 roadways to the BRDA and/or storage embankments (Evans, 2016). However, finding
80 appropriate options for the re-use of the fine fraction bauxite residue remains elusive (Power
81 et al., 2011; IAI, 2015).
82
83 Fine fraction bauxite residue comprises Fe oxides (20-45%) and aluminium (Al) oxides (10-
84 22%) (IAI 2015), which make it suitable as a medium to adsorb phosphorus (P). The
85 European Commission (EC) has identified waste management as an important aspect of the
86 "circular economy" (EC, 2015), so in recent years, emphasis has been placed on investigating
87 alternative methods of P recovery from wastewater (Grace et al., 2015, 2016). A move from
88 the more conventional methods of P recovery such as biological removal and chemical
89 precipitation (Wang et al., 2008), to the use of low-cost adsorbents from industrial solid
90 wastes, such as bauxite residue, have been examined. In comparison to standard P removal
91 by sand, bauxite residue has a high P retention capacity (Vohla et al., 2007). However, its P
92 removal potential is enhanced following treatment by heat, acid or gypsum (Table 1). Of the
93 methods employed, acid and heat treatment have proved most successful in increasing the P
94 adsorption capacity of the bauxite residue, with maximum adsorption capacities of up to 203
95 mg P g^{-1} bauxite being achieved (Liu et al., 2007) compared to untreated residue (0.20 mg P
96 g^{-1}; Grace et al., 2015) (Table 1). However, whilst acid and heat treatments have proven to be
97 very successful in increasing the adsorption capacity of bauxite residue, they are expensive,
98 energy consuming (using high temperatures up to 700˚C) (Xue et al., 2016), and, without
99 further treatment, do not allow for the easy reuse of the bauxite residue (e.g. as a possible
100 media for plant growth) (Xue et al., 2016).
101

Treatments such as seawater or gypsum provide relatively inexpensive, alternative treatments, which may not only enhance the P adsorption capacity of the bauxite residue media, but may also help to improve its physicochemical characteristics. Seawater treatment improves bauxite's physical structure, due to the addition of magnesium (Mg) and calcium (Ca) which behave as flocculating agents, allowing many of the fine particles in bauxite residue to form more stable aggregates (Jones and Haynes, 2011), and a partial decrease in sodium (Na) due to ion exchange with Mg, Ca and potassium (K) (Hanahan et al., 2004). Seawater-treated bauxite residues also allow adsorbed P to become bio-available, unlike the metal cations which are unavailable, highlighting the P and metal retention capabilities (Fergusson, 2009). Revegetation of bauxite residue using gypsum has also improved plant growth by reducing its alkalinity and salinity, and improving the structure of the residue (Courtney et al., 2009; Courtney and Kirwan, 2012). In addition to this, modern alumina refineries are often located close to deep water ports, to allow for the bulk shipment of incoming bauxite (sometimes from multiple sources) to the refinery and/or for bulk shipment of alumina to aluminium smelters situated elsewhere. Therefore, there is ample scope for the increasing use of seawater neutralization technology for pre-treatment of residues in refineries not already employing treatments previously mentioned, prior to their deposition in the BRDA.

To the best of the authors' knowledge, no study has previously compared the use of raw seawater or gypsum treatments on the separate fractions of bauxite residue as a method of neutralisation and preparation for the re-use of bauxite residue in its separated and unseparated fractions as low-cost adsorbents and a potential source of P. The objectives of this study were to (1) characterise bauxite residue from two different sources, before and after treatment with seawater and gypsum, and to investigate their potential to release trace

127 elements (2) investigate the effect of the treated bauxite residue on P adsorption (3) assess the
128 impact of particle size, mineral and elemental (particularly Ca and Mg) composition of the
129 bauxite residue on the adsorption of P.
130
131 **2. Materials and Methods**
132
133 2.1 Sample preparation
134 A one kilogram, sample of fresh bauxite residue was obtained from Alteo Gardanne
135 [Gardanne, France (43˚27'9"N, 5˚27'41" E)], who operate a co-disposal method for fine and
136 coarse fractions of bauxite. This sample will be referred to hereafter as UFR. One kilogram
137 of mud-farmed bauxite residue samples (treated by atmospheric carbonation and therefore
138 non-hazardous), were also obtained from Rusal Aughinish Alumina [Limerick, Ireland
139 (52˚37'06"N, 9˚04'19"W)], who separate the fine (particle sizes <100 µm) and coarse
140 (particle sizes >150 µm) fraction of bauxite residue before disposal (IAI 2015) in a ratio of
141 9:1 (fine: coarse). The fine and coarse fractions will be referred to hereafter as UF (untreated
142 fine) and UC (untreated coarse).
143
144 Before any analysis or experiments were conducted, all bauxite residue samples were dried at
145 105˚C for 24 hr. Once dry, the samples were pulverised using a mortar and pestle and sieved
146 to a particle size <2 mm. 0.3 kg of each sample were then treated with either seawater (S) or
147 laboratory-grade gypsum (G) (Lennox, Ireland), so two treatments were applied to each
148 source of bauxite residue. S or G, placed after the above abbreviations, indicates the
149 treatment applied. Gypsum was applied to the 0.3 kg bauxite residue samples at a ratio of 8%
150 (w/w) (Lopez et al., 1998) and leached for 72 hr in accordance with standard methods (BSI,
151 2002). Seawater amendment involved mixing with 0.3 kg bauxite at a ratio of 5:1 (v/w)

(after Johnston et al., 2010), for 1 hr, followed by a 12 hr settlement period overnight. The bauxite residue and seawater mixture was then filtered through a 0.45 μm membrane using a vacuum pump. The treated bauxite residue samples were then oven dried for 24 hr, pulverised with a mortar and pestle, and sieved to <2 mm in size.

2.2 Characterisation Study

Untreated and treated bauxite samples were characterised (n=3) for their physical, chemical, elemental and mineralogical properties. Soil pH and electrical conductivity (EC) were measured in an aqueous extract, using 5 g of bauxite residue sample in a 1:5 ratio (solid: liquid) (Courtney and Harrington, 2010). The bulk density (ρ_b) was determined after Blake (1965) and the particle density (ρ_p) after Blake and Hartge (1986) using 10 g of bauxite residue samples. Total pore space (S_t) was calculated using the values obtained for the bulk and particle densities (Danielson and Sutherland, 1986). The effective particle size analysis (PSA) was determined on particle sizes <53 μm using optical laser diffraction on the Malvern Zetasizer 3000HS® (Malvern, United Kingdom) with online autotitrator and a Horiba LA-920, and reported at specific cumulative % (10, 50 and 90%). Mineralogical detection was carried out using X-ray diffraction (XRD) on 1 g samples using a Philips X'Pert PRO MPD® (California, USA), whilst surface morphology and elemental detection were carried out using scanning electron microscopy (SEM) and energy-dispersive X-ray spectroscopy (EDS) on a Hitachi SU-70 (Berkshire, UK), using approximately 1 g samples. Quantification of the elemental content was carried out on 1 g samples by Brookside Laboratories (OH, USA) after digestion (EPA, 1996) using Inductively Coupled Plasma Atomic Emission Spectroscopy (ICP-AES) and elemental composition quantified using X-ray fluorescence (XRF). Measurement of the point of zero charge (PZCpH) was after Vakros et al. (2002) using 1 g samples, and cation exchange capacity (CEC) was determined using the K saturation

technique (Thomas, 1982), using 5 g samples. Brunauer-Emmett-Teller specific surface area (SSA) and pore volume analysis were conducted on 1 g samples, which were degassed at 120ºC for 3 hr prior to analysis carried out by Glantreo Laboratories (Cork, Ireland).

2.3 Phosphorus Adsorption Batch Study

The P adsorption capacity of nine bauxite samples (untreated and gypsum/seawater treated samples) were examined in a bench-scale experiment. To conduct a P adsorption isotherm test, ortho-phosphorus (PO_4^{3-}-P) solutions were made up to known concentrations using potassium dihydrogen phosphate (K_2HPO_4) in distilled water. One gram of each of the sieved media was placed into a series of 50 ml-capacity containers and was overlain with 25 ml of the solutions. Each sample was then shaken in a reciprocal shaker at 250 rpm for 24 hr. At t = 24 hr, the supernatant water from each sample container was filtered using 0.45µm filters and analysed immediately using a nutrient analyser (Konelab 20, Thermo Clinical Labsystems, Finland). The data obtained from the P adsorption batch studies were modelled using the Langmuir adsorption isotherm (McBride, 2000), which assumes monolayer adsorption on adsorption sites and allows for the estimation of the maximum P adsorption capacity (q_{max}) of the media:

$$q_i = q_{max}\left(\frac{k_a\, C_e}{1 + k_a\, C_e}\right) \quad (1)$$

where q_i is the quantity of the contaminant adsorbed per gram of media (g g^{-1}), C_e is the equilibrium contaminant concentration in the water (g m^{-3}), k_a is a measure of the affinity of the contaminant for the media (m^3 g^{-1}), and q_{max} is the maximum amount of the contaminant that can be adsorbed onto the media (g g^{-1}).

201

202 2.3.1. Mobilization of Metals

203 To determine whether the residue media released trace elements, 25 mL of water was mixed
204 with 1 g of media for 24 hr and the supernatant was analysed by ICP-MS. The elements
205 selected for detection were Al, arsenic (As), barium (Ba), beryllium (Be), boron (B),
206 cadmium (Cd), Ca, chromium (Cr), copper (Cu), Fe, gallium (Ga), K, lead (Pb), Mg,
207 manganese (Mn), mercury (Hg), molybdenum (Mo), Na, nickel (Ni), P, selenium (Se), silicon
208 (Si), titanium (Ti), vanadium (V), and zinc (Zn).

209

210 2.4 Statistical analysis

211 Linear regression analysis was utilised to examine the extent of correlation between the
212 individual characteristic parameters of the bauxite residue samples and bauxite adsorption,
213 using Minitab. A Pearson correlation coefficient and a correlation p-value were determined to
214 quantify correlation. The p-value represents the probability that the correlation between the
215 bauxite residue characteristic in question and the response variable (adsorption) is zero i.e.
216 the probability that there is no relationship between the two.

217

218 **3. Results and Discussion**

219

220 3.1 Characterisation of bauxite residue

221

222 3.1.1 Effect of treatments on elemental and mineralogical composition

223 The mineral and total elemental composition of the three untreated bauxite residues [UF
224 (untreated fine fraction), UC (untreated coarse fraction), and UFR (untreated co-disposed)]
225 are shown in Tables 2 and 3. Bauxite residues are typically high in Fe and Al oxides (Liu et

226 al., 2007), which was found to be the case in this study. The mineralogical composition
227 present for all untreated samples was dominated by Fe_2O_3, Al_2O_3, SiO_2 and CaO. A decrease
228 in Al_2O_3 was noted following treatment with the gypsum and the seawater in all samples,
229 with an increase in CaO content noted in samples treated with gypsum.
230
231 XRD analysis showed that the main crystalline phases present in UF were haematite (Fe_2O_3),
232 goethite (FeO(OH)), perovskite ($CaTiO_3$), boehmite (AlO(OH)), rutile (TiO_2), gibbsite
233 $Al(OH)_3$ and sodalite $Na_8(Al_6Si_6O_{24})Cl_2$ (Figure S1 in the Supplementary Material).
234 Similarly, the main minerals in UFR were haematite (Fe_2O_3), goethite (FeO(OH)), boehmite
235 (AlO(OH)), rutile (TiO_2), gibbsite $Al(OH)_3$ and sodalite $Na_8(Al_6Si_6O_{24})Cl_2$ (Figure S2).
236 Boehmite (AlO(OH)), rutile (TiO_2), gibbsite $Al(OH)_3$ haematite (Fe_2O_3) were the
237 predominant minerals present in UC (Figure S3). Following treatment with seawater and
238 gypsum, a change in mineral phase in UFG, UFS, UFRS and UFRG occurred (Figure S4, S5,
239 S6, S7). After treatment with gypsum, a higher presence of the calcium carbonate, calcite
240 ($CaCO_3$), was detected in UFRG and UCG (Figure S7 and S8), and post seawater treatment,
241 small peaks representing brucite ($Mg(OH)_2$ were detected in UFS and UCS (S5 and S9).
242
243 These findings are similar to previous studies that examined various neutralization techniques
244 for bauxite residue (Gräfe et al., 2009). When seawater is added to bauxite residue, a reaction
245 occurs where the hydroxide, carbonate and aluminate ions are eliminated due to a reaction
246 involving Mg^{2+} and Ca^{2+} (from the seawater) (Gräfe et al., 2009; Palmer and Frost, 2009).
247 This results in the formation of alkaline solids such as the calcium carbonates, calcite and
248 brucite, which cause a buffering effect, evidenced in a shift of pH to between 8 and 9 (Power
249 et al., 2011). The addition of gypsum ($CaSO_4$) results in a drop in the pH (approximately 8.6)
250 due to the precipitation of excess hydroxides (OH-), aluminium hydroxides ($Al(OH)_4^-$),

carbonates (CO_3^{2-}) to form calcium hydroxide/lime (Ca(OH)), tri-calcium aluminate (TCA), hydrocalumite and calcium carbonate ($CaCO_3$), which behave as buffers and maintain pH (Gräfe et al., 2009). The addition of Ca also flocculates and helps with the formation of more stable aggregates (Jones and Haynes, 2011).

An analysis of water samples (Table S1) to examine mobilisation of metals showed that As, Al and Cr were present in the leachate from the UFR sample, but decreased following gypsum and seawater treatments. Arsenic, Fe and Al were mobilised from the UF sample, but these concentrations were reduced following treatment with gypsum and seawater. Aluminium was mobilised from the UC. The reduction in Fe and Al following treatment with either gypsum or seawater is in line with previous studies, which have shown that water soluble Fe and Al decrease following gypsum application (Courtney and Timpson, 2005). Overall, Al still remained above the maximum allowable concentration (MAC) of 0.2 mg L^{-1} (200 µg L^{-1}) (EPA, 2014) for Al for drinking water. Sodium was still at a high level following gypsum and seawater treatments, ranging from 139.3±3.2 to 153±24.8 mg L^{-1} and 241.3±26 to 388.7±18.6 mg L^{-1}, respectively. The MAC for Na in drinking water is 200 mg L^{-1} (EPA, 2014).

3.1.2 Effect of treatments on physicochemical properties

The untreated bauxite residues had high pH (10.8±0.12 to 11.9±0.06) and EC (704±90.8 to 1184±48.8µS cm^{-1}) (Table 4). Following treatment with gypsum and seawater, pH decreased and EC increased. Changes for pH after treatment with either seawater or gypsum are due to precipitation of calcium carbonates such calcite, brucite and aragonite, which behave as buffers and maintain a reduced pH (Menzies et al., 2004), while the increase in EC is attributed to the introduction of excess Na^+ and Ca^{2+} (Gräfe et al., 2009). The pH of bauxite

276 residue is normally within the range of 11 to 13 (Newson et al., 2006), but varies due to the
277 type of bauxite ore, Bayer process, and neutralisation techniques used in the refinery. Both
278 seawater (Menzies et al., 2004; Johnston et al., 2010) and gypsum applications (Jones and
279 Haynes, 2011; Courtney and Kirwan, 2012; Lehoux et al., 2013) are recognised methods of
280 reducing the alkalinity of bauxite residues.
281
282 No change was observed in the particle size or particle size density following the addition of
283 the gypsum and seawater treatments to the various bauxite residue samples (Table 4).
284 Similarly, the addition of gypsum or seawater did not have any impact on bulk density (Table
285 4).
286
287 The surface morphology of bauxite residues typically comprises 30% amorphous and 70%
288 crystalline phase (Gräfe et al., 2009). However, in this study SEM imaging suggests that the
289 bauxite residue samples were not present in strong crystalline form (Figure 1), in particular
290 for samples UF and UFR, as no distinctive crystalline structure to the bauxite residue samples
291 was observed. Liu et al. (2007) examined the effect of age on stored bauxite residue, and
292 found that fresh bauxite residue particles are present in poorly formed crystallised or
293 amorphous form in comparison to older bauxite residue (10 years), which has a stronger
294 crystalline formation, indicating that crystallisation occurs in some of the minerals over time.
295 As the bauxite residue used in this study was fresh, this would explain why there was not a
296 strong distinction between amorphous or crystalline forms, similar to the findings of Liu et al.
297 (2007). The composition of fine particles and larger particles in the coarse fraction (UC) were
298 noticeable from the SEM (Figure 1).
299

300 Improved aggregate formation was noticeable in the gypsum and seawater-treated bauxite
301 residues (Figure 1), due to the addition of Ca^{2+}, which results in flocculation (Zhu et al.,
302 2016). Changes in the surface morphology were also evident in the gypsum and seawater-
303 treated residues in comparison to the untreated residues, which appeared to have a much
304 smoother surface (Figure 1). This change in surface morphology following the treatments
305 was attributed to the changes in mineral phase (Huang et al., 2008).
306
307 3.2 Phosphorus Adsorption Study
308
309 3.2.1 Effect of seawater and gypsum treatment on P adsorption
310 All nine bauxite residue samples in this study were successful in removing P from aqueous
311 solution (Table 5). Bauxite residue has been shown in numerous P adsorption studies to have
312 a high P retention capacity, particularly following treatment or modification (Ye et al., 2014;
313 Grace et al., 2015). In this study, gypsum or seawater treatment had a positive impact on P
314 removal, with the gypsum-treated bauxite residue performing best (Table 5).
315
316 Following seawater treatment, the P adsorption capacity of the bauxite residues increased to
317 q_{max} values of 0.48, 0.66 and 1.92mg P g^{-1} media for UFS, UCS and UFRS, respectively. In
318 previous studies, following treatment with seawater, bauxite residue had a higher adsorption
319 capacity for P. Akhurst et al. (2006) reported a maximum adsorption of 6.5 mg P g^{-1} when
320 using a bauxite residue treated with brine (Bauxsol™). This relatively high adsorption may
321 be attributed to the higher concentrations of Ca^{2+} and Mg^{2+} in the brines (or products such as
322 Bauxsol™, developed by Basecon™), in comparison to raw seawater (0.41, 1.29 and 10.77g
323 kg^{-1} of Ca^{2+}, Na and Mg^{2+}, respectively) used in this study (Gräfe et al., 2009). The gypsum-
324 treated bauxite residues had the highest q_{max} values – 2.46, 1.39 and 2.73mg P g^{-1} media for

325 UFG, UCG and UFRG, respectively. However, these values were lower than a P adsorption
326 study carried out by Lopez et al. (1998), who used the same application rate of gypsum to the
327 bauxite residue samples and reported a q_{max} of 7.03 mg P g^{-1}. The lower rate observed in the
328 current study may be attributed to the 72 hr leaching process that the gypsum-treated bauxite
329 residue underwent before use in the adsorption study, which may have allowed for further
330 exchange and removal of Ca^{2+} following the leaching process.
331
332 Overall, the bauxite residue in the current study had a higher P adsorbency than in other
333 studies for zeolite (0.01 mg P g^{-1}, Grace et al., 2015) and granular ceramics (0.9 mg g^{-1}; Chen
334 et al., 2012), but lower than fly ash, granular blast furnace slag and pyritic fill (6.48, 3.61 and
335 0.88 mg P g^{-1}, respectively; Grace et al., 2015), crushed concrete (19.6 mg P g^{-1}; Egemose et
336 al., 2012), untreated biochar (32 mg P g^{-1}; Wang et al., 2015), and NaOH-modified coconut
337 shell powder (200 mg P g^{-1}; de Lima et al., 2012).
338
339 3.2.2 Factors affecting P adsorption
340 The adsorption of P onto media is influenced by many factors which include particle size, pH,
341 component and surface characteristics (Wang et al., 2016). Numerous studies have
342 investigated the effect of parameters such as kinetics of P adsorption (Akhurst et al., 2006;
343 Liu et al., 2007; Ye et al., 2014; Grace et al., 2015), ionic solution (Akhurst et al., 2006), pH
344 (Liu et al., 2007; Huang et al., 2008; Grace et al., 2015) on the adsorption of P from aqueous
345 solution. While all bauxite residue samples in this study did remove P from aqueous solution,
346 it is clear that the application of treatments, such as gypsum or seawater, has an effect on the
347 adsorption capability, and that the rate of adsorption will vary as a result of the source of
348 bauxite residue and treatments used (Wang et al., 2008).
349

350 The parameters which showed a statistically significant positive correlation of medium
351 strength with P adsorption in this study were Ca (correlation coefficient = 0.47, p = 0.01,
352 Degrees of Freedom (DoF) = 25) and CaO (correlation coefficient = 0.39, p = 0.04, DoF =
353 25). A statistically significant negative correlation of medium strength was also detected
354 between pH and P adsorption (correlation coefficient = - 0.38, p = 0. 05, DoF = 25). pH was
355 a contributing factor to the adsorption process with the amount of phosphate adsorbed
356 increasing with a decrease in pH in the media following treatments, UFRG>UFRS>UFR,
357 UFG>UFS>UF, UCG>UCS>UC. This was a similar finding to several studies carried out
358 (Li et al., 2006; Liu et al., 2007; Huang et al., 2008; Grace et al., 2015). The Ca ions also
359 influenced P adsorption. This is as a result of the high level of Ca^{2+} and Mg^{2+} present in the
360 bauxite residue, particularly after seawater and gypsum treatments, when the majority of
361 PO_4^{3-} is removed from solution due to the formation of magnesium phosphate ($Mg_3(PO_4)_2$)
362 and calcium phosphate ($Ca_3(PO_4)_2$) (Akhurst et al., 2006).
363
364 The pH at which net charges are neutral on the surface of the adsorbent - the point of zero
365 charge (PZC) - influences the rate of adsorption of P (Jacukowicz-Sobala et al., 2015). Where
366 the pH is higher than the PZCpH, the surface of the adsorbent media becomes more negative
367 (attracting more cations), as a result of the adsorption of OH^- from the surrounding solution
368 (Prajapati et al., 2016). The PZCpH ranged from 6.16±0.21 to 6.96±1.21 (Table 4) in the
369 three untreated samples. Following treatment with gypsum and seawater, there were notable
370 changes, but no statistical relevance was detected between the PZCpH and P adsorption in
371 this study. However, as bauxite residue is composed of numerous minerals, each with their
372 own individual PZCpH (which, as noted in the literature, can range from anywhere between
373 pH 2 to pH 9.8 (Gräfe et al., 2009)), this results in the bauxite residue being able to cater for a

374 wide range of pH (Gräfe et al., 2009) and also having the capability of removing both cations
375 and anions from solution.
376
377 The SSA analysis carried out on the bauxite residues show an increase in specific surface
378 area in all samples following treatment with either the gypsum or the seawater (Table 4).
379 There was also an increase in pore volume following the addition of either gypsum or
380 seawater (Table 4). This is attributed to the formation of precipitates formed in the
381 neutralisation process of both gypsum and seawater and the effect of the Ca acting as a
382 flocculant with the finer particles present. This increase in surface area also contributes to the
383 increase in P adsorption following treatments. Although particle size affects adsorption onto
384 media, due to the availability of sites for P uptake, no significant correlation was observed in
385 the current study.
386
387 3.3 Implications of the findings of this study
388 The use of gypsum and seawater treatments on bauxite residue improved the overall P
389 adsorption capacity of the bauxite residue samples, but mixing the bauxite residue and
390 treatments with actual wastewater will be necessary to fully understand the total adsorption
391 behaviour of the bauxite residue. In addition to improving the P adsorption, alkalinity was
392 significantly reduced following both treatments; however, the EC was increased. This may
393 limit the growth of plants on the gypsum or seawater-treated bauxite residues; therefore, one
394 option may be to increase the rinsing period of the bauxite residue following treatment to
395 remove the excess Ca^{2+} and Na^{+} ions in solution. Lowering the alkalinity, increasing the P,
396 Ca^{2+} and Mg^{2+} content and improving the physical structure, provide the possible re-use
397 option of using the treated bauxite residue as a growth media.
398

For a refinery, the cost of neutralisation techniques is an obvious consideration when deciding which technique(s) to use. The use of seawater as a neutralisation technique would be a cheap and feasible option for a refinery that is close to the sea. The establishment of a pipeline (if not already in place) would be the dominant capital cost. The use of a Nano filtration system to concentrate the Ca^{2+}, Mg^{2+} and Na^{+} ions in the seawater (Couperthwaite et al., 2014) could allow for the reduction in volume of seawater necessary for the neutralisation process, but may add to the cost. Gypsum however may be a more expensive option, requiring machinery such as amphirolls for the mixing and spreading of the gypsum. However, depending on the refinery's location, waste gypsum from construction sites or fossil fuel powered power stations may be used (Jones and Haynes, 2011).

4. Conclusions

This study examined the impact of gypsum and seawater treatments on the mineral, elemental and physiochemical properties of bauxite residue. The untreated bauxite residues were high in Fe and Al oxides and their mineralogical composition was dominated by Fe_2O_3, Al_2O_3, SiO_2 and CaO. Following treatment with gypsum and seawater, the pH decreased and EC increased, but no change was observed in the particle size or density. The SSA and pore volume of the bauxite increased following both treatments, which contributed to increased P adsorbency. Although the P adsorbency measured in this study was not as high as measured in other studies using different media, it still indicates that reuse in water or wastewater treatment facilities may be an appropriate option for bauxite residue.

Acknowledgements

The authors would like to acknowledge the financial support from the Irish Environmental Protection Agency (EPA) (2014-RE-MS-1) and the UK Natural Environment Research Council (NE/L01405X/1). The authors would also like to thank Rusal Aughinish Alumina and Alteo Gardanne, who provided the bauxite residue sand and mud samples.

448 **References**

449

450 Akhurst, D.J., Jones, G.B., Clark, M., McConchie, D., 2006. Phosphate removal from
451 aqueous solutions using neutralised bauxite refinery residues (Bauxsol™). Environ. Chem. 3,
452 65-74.

453

454 Blake, G.R., 1965. Bulk density, in: Black, C.A. (Ed), Methods of soil analysis. Part 1.
455 Physical and mineralogical properties, including statistics of measurement and sampling.
456 ASA, SSSA, Madison, WI, pp. 374 – 390.

457

458 Blake, G.R., Hartge, K.H., 1986. Particle density, in: Klute, A. (Ed), Methods of Soil
459 Analysis: Part 1—Physical and Mineralogical Methods. SSSA, ASA, Madison, WI, pp. 377 –
460 382.

461

462 British Standard Institution, 2002. 12457-2. Characterisation of waste. Leaching. Compliance
463 test for leaching of granular waste materials and sludges. One stage batch test at a liquid to
464 solid ratio of 10 l/kg for materials with particle size below 4 mm (without or with size
465 reduction).

466

467 Chen, N., Feng, C., Zhang, Z., Liu, R., Gao, Y., Li, M.,Sugiura, N., 2012. Preparation and
468 characterization of lanthanum (III) loaded granular ceramic for phosphorus adsorption from
469 aqueous solution. J. Taiwan Instit. Chem. Eng. 43, 783-789.

470

471 Cooling, D.J., 2007. Improving the sustainability of residue management practices-Alcoa
472 World Alumina Australia. In: (A. Fouri and R.J. Jewell, Eds) Paste and Thickened Tailings:

A Guide, 316.
http://citeseerx.ist.psu.edu/viewdoc/download?doi=10.1.1.629.1067&rep=rep1&type=pdf. (accessed 31.10.17).

Couperthwaite, S.J., Johnstone, D.W., Mullett, M.E., Taylor, K.J., Millar, G.J., 2014. Minimization of bauxite residue neutralization products using nanofiltered seawater. Ind. Eng. Chem. Res. 53, 3787-3794.

Courtney, R.G., Timpson, J.P., 2005. Reclamation of fine fraction bauxite processing residue (red mud) amended with coarse fraction residue and gypsum. Water Air Soil Poll. 164(1-4), 91-102.

Courtney, R.G., Jordan, S.N., Harrington, T., 2009. Physico- chemical changes in bauxite residue following application of spent mushroom compost and gypsum. Land. Degrad. Dev. 20, 572-581.

Courtney, R., Harrington, T., 2010. Assessment of plant-available phosphorus in a fine textured sodic substrate. Ecol. Eng. 36, 542-547.

Courtney, R., Kirwan, L., 2012. Gypsum amendment of alkaline bauxite residue–plant available aluminium and implications for grassland restoration. Ecol. Eng. 42, 279-282.

Danielson, R.E., Sutherland, P.L., 1986. Porosity, in: Klute, A. (Ed), Methods of soil analysis. Part 1. Physical and Mineralogical Methods. SSSA, ASA, Madison, WI, pp. 443-461.

498

499 de Lima, A.C.A., Nascimento, R.F., de Sousa, F.F., Josue Filho, M., Oliveira, A.C., 2012.
500 Modified coconut shell fibers: a green and economical sorbent for the removal of anions from
501 aqueous solutions. Chem. Eng. J. 185, 274-284.

502

503 Dilmore, R.M., Howard, B.H., Soong, Y., Griffith, C., Hedges, S.W., DeGalbo, A.D.,
504 Morreale, B., Baltrus, J.P., Allen, D.E., Fu, J.K., 2009. Sequestration of CO2 in mixtures of
505 caustic byproduct and saline waste water. Environ. Eng. Sci. 26, 1325-1333.

506

507 Eastham J, Morald T, Aylmore P., 2006. Effective nutrient sources for plant growth on
508 bauxite residue. Water Air Soil Poll. 176(1–4),5–19

509

510 Egemose, S., Sønderup, M.J., Beinthin, M.V., Reitzel, K., Hoffmann, C.C., Flindt, M.R.,
511 2012. Crushed concrete as a phosphate binding material: a potential new management tool. J.
512 Environ. Qual. 41, 647-653.

513

514 EPA, 1996. EPA Method 3050B: Acid Digestion of Sediments, Sludges, and Soils.
515 www.epa.gov/sites/production/files/2015-06/documents/epa-3050b.pdf (accessed
516 30.10.2017).

517

518 EPA, 2014. Drinking Water Parameters Microbiological, Chemical and Indicator Parameters
519 in the 2014 Drinking Water Regulations.
520 www.epa.ie/pubs/advice/drinkingwater/2015_04_21_ParametersStandaloneDoc.pdf
521 (accessed 30.10.2017).

522

523 European Commission, 2015. COM 2015. 614 Communication from the commission to the
524 European Parliament, the Council, the European Economic and Social Committee and the
525 Committee of the regions - Closing the loop - An EU action plan for the circular economy.
526 Brussels.
527
528 Evans, K., 2016. The history, challenges, and new developments in the management and use
529 of bauxite residue. J. Sustain. Metallurgy 2, 316-331.
530
531 Fergusson, L., 2009. Commercialisation of environmental technologies derived from alumina
532 refinery residues: A ten-year case history of
533 Virotec. http://citeseerx.ist.psu.edu/viewdoc/download?doi=10.1.1.458.2073&rep=rep1&typ
534 e=pdf (accessed 8.12.17)
535
536 Fois, E., Lallai, A., Mura, G., 2007. Sulfur dioxide absorption in a bubbling reactor with
537 suspensions of Bayer red mud. Ind. Eng. Chem. Res. 46, 6770-6776.
538
539 Grace, M.A., Healy, M.G., Clifford, E., 2015. Use of industrial by-products and natural
540 media to adsorb nutrients, metals and organic carbon from drinking water. Sci. Total.
541 Environ. 518, 491-497.
542
543 Grace, M.A., Clifford, E., Healy, M.G., 2016. The potential for the use of waste products
544 from a variety of sectors in water treatment processes. J. Clean. Prod.137, 788-802.
545

546 Goloran, J.B., Chen, C.R., Phillips, I.R., Xu, Z.H., Condron, L.M., 2013. Selecting a nitrogen
547 availability index for understanding plant nutrient dynamics in rehabilitated bauxite-
548 processing residue sand. Ecol. Eng. 58, 228-237.
549
550 Gräfe, M., Power, G., Klauber, C., 2009. Review of bauxite residue alkalinity and associated
551 chemistry. CSIRO, Australia.
552 http://enfo.agt.bme.hu/drupal/sites/default/files/vörösiszpa%20kémia%20és%20lúgosság.pdf
553 (accessed 12.12.17)
554
555 Hanahan, C., McConchie, D., Pohl, H.,, Creelman, R., Clark, M., Stocksiek C., 2004.
556 Chemistry of seawater neutralization of bauxite refinery residues (red mud). Environ. Eng.
557 Sci. 21,125–138
558
559 Huang, W., Wang, S., Zhu, Z., Li, L., Yao, X., Rudolph, V., Haghseresht, F., 2008.
560 Phosphate removal from wastewater using red mud. J. Hazard. Mater. 158, 35-42.
561
562 IAI, 2015. Bauxite residue management: best practice. http://www.world-
563 aluminium.org/media/filer_public/2015/10/15/bauxite_residue_management_-
564 _best_practice_english_oct15edit.pdf. (accessed 14.10.2017).
565
566 Jacukowicz-Sobala, I., Ociński, D., Kociołek-Balawejder, E., 2015. Iron and aluminium
567 oxides containing industrial wastes as adsorbents of heavy metals: Application possibilities
568 and limitations. Waste. Manage. Res. 33, 612-629.
569

570 Johnston, M., Clark, M.W., McMahon, P., Ward, N., 2010. Alkalinity conversion of bauxite
571 refinery residues by neutralization. J. Hazard. Mater. 182, 710-715.
572
573 Jones, B.E., Haynes, R.J., 2011. Bauxite processing residue: a critical review of its formation,
574 properties, storage, and revegetation. Crit. Rev. in Env. Sci. Tec 41, 271-315.
575
576 Jones, B.E., Haynes, R.J., Phillips, I.R., 2012. Addition of an organic amendment and/or
577 residue mud to bauxite residue sand in order to improve its properties as a growth medium. J.
578 Environ. Manage. 95, 29-38.
579
580 Kirwan, L.J., Hartshorn, A., McMonagle, J.B., Fleming, L., Funnell, D., 2013. Chemistry of
581 bauxite residue neutralisation and aspects to implementation. Int. J. Miner. Process. 119, 40-
582 50.
583
584 Klauber, C., Gräfe, M., Power, G., 2011. Bauxite residue issues: II. options for residue
585 utilization. Hydrometallurgy 108, 11-32.
586
587 Lehoux, A.P., Lockwood, C.L., Mayes, W.M., Stewart, D.I., Mortimer, R.J., Gruiz, K.,
588 Burke, I.T., 2013. Gypsum addition to soils contaminated by red mud: implications for
589 aluminium, arsenic, molybdenum and vanadium solubility. Environ. Geochem. Hlth 35, 643-
590 656.
591
592 Li, L.Y., 2001. A study of iron mineral transformation to reduce red mud tailings. Waste
593 Manage 21, 525-534.
594

595 Li, Y., Liu, C., Luan, Z., Peng, X., Zhu, C., Chen, Z., Zhang, Z., Fan, J., Jia, Z., 2006.
596 Phosphate removal from aqueous solutions using raw and activated red mud and fly ash. J.
597 Hazard. Mater. 137, 374-383.
598
599 Liu, Y., Lin, C., Wu, Y., 2007. Characterization of red mud derived from a combined Bayer
600 Process and bauxite calcination method. J. Hazard. Mater. 146, 255-261.
601
602 Liu, W., Chen, X., Li, W., Yu, Y., Yan, K., 2014. Environmental assessment, management
603 and utilization of red mud in China. J. Clean. Prod. 84, 606-610.
604
605 Lopez, E., Soto, B., Arias, M., Nunez, A., Rubinos, D., Barral, M.T., 1998. Adsorbent
606 properties of red mud and its use for wastewater treatment. Water. Res. 32, 1314-1322.
607
608 Mayes, W.M., Burke, I.T., Gomes, H.I., Anton, A.D., Molnár, M., Feigl, V., Ujaczki, É.,
609 2016. Advances in understanding environmental risks of red mud after the Ajka spill,
610 Hungary. J. Sustain. Metallurgy. 2, 332-343.
611
612 Menzies, N.W., Fulton, I.M., Morrell, W.J., 2004. Seawater neutralization of alkaline bauxite
613 residue and implications for revegetation. J. Environ. Qual. 33, 1877-1884.
614
615 McBride, M.B., 2000. Chemisorption and precipitation reactions. Handbook of Soil Science.
616 CRC Press, Boca Raton, FL, B265-B302.
617
618 McConchie, D., Clark, M., Davies-McConchie, F., 2001. Processes and Compositions for
619 Water Treatment, Neauveau Technology Investments, Australian, p. 28.

620 Newson, T., Dyer, T., Adam, C., Sharp, S., 2006. Effect of structure on the geotechnical
621 properties of bauxite residue. J. Geotech. Geoenviron. 132, 143-151.
622
623 Palmer, S.J., Frost, R.L., 2009. Characterisation of bauxite and seawater neutralised bauxite
624 residue using XRD and vibrational spectroscopic techniques. J. Mater. Sci. 44, 55-63.
625
626 Power, G., Gräfe, M., Klauber, C., 2011. Bauxite residue issues: I. Current management,
627 disposal and storage practices. Hydrometallurgy 108, 33-45.
628
629 Pradhan, J., Das, S.N., Das, J., Rao, S.B., Thakur, R.S., 1996. Characterization of Indian red
630 muds and recovery of their metal values. Annual meeting and exhibition of the minerals,
631 metals and materials society, Anaheim, CA, 4 – 8 February 1996.
632
633 Prajapati, S.S., Najar, P.A., Tangde, V.M., 2016. Removal of Phosphate Using Red Mud: An
634 Environmentally Hazardous Waste By-Product of Alumina Industry. Adv. Phy. Chemistry,
635 2016.
636
637 Snars, K., Gilkes, R.J., 2009. Evaluation of bauxite residues (red muds) of different origins
638 for environmental applications. Appl. Clay. Sci. 46, 13-20.
639
640 Thomas, G.W., 1982. Exchangeable cations. Methods of soil analysis. Part 2. Chemical and
641 microbiological properties, (methodsofsoilan2), 159-165.
642
643 Vakros, J., Kordulis, C., Lycourghiotis, A., 2002. Potentiometric mass titrations: a quick scan
644 for determining the point of zero charge. Chem. Commun. 17, 1980-1981.

645

646 Vohla, C., Alas, R., Nurk, K., Baatz, S., Mander, Ü., 2007. Dynamics of phosphorus,
647 nitrogen and carbon removal in a horizontal subsurface flow constructed wetland. Sci. Tot.
648 Environ. 380, 66-74.
649
650 Wang, S., Ang, HM., Tadé, M.O., 2008. Novel applications of red mud as coagulant,
651 adsorbent and catalyst for environmentally benign processes. Chemosphere 72, 1621–1635
652
653 Wang, B., Lehmann, J., Hanley, K., Hestrin, R., Enders, A., 2015. Adsorption and desorption
654 of ammonium by maple wood biochar as a function of oxidation and pH. Chemosphere 138,
655 120-126.
656
657 Wang, Z., Shen, D., Shen, F., Li, T., 2016. Phosphate adsorption on lanthanum loaded
658 biochar. Chemosphere 150, 1-7.
659
660 Xue, S., Zhu, F., Kong, X., Wu, C., Huang, L., Huang, N., Hartley, W., 2016. A review of the
661 characterization and revegetation of bauxite residues (Red mud). Environ. Sci. Poll. Res. 23,
662 1120-1132.
663
664 Ye, J., Zhang, P., Hoffmann, E., Zeng, G., Tang, Y., Dresely, J., Liu, Y., 2014. Comparison
665 of response surface methodology and artificial neural network in optimization and prediction
666 of acid activation of Bauxsol for phosphorus adsorption. Water Air Soil Poll. 225(12), 2225.
667

668 Zhu, F., Li, Y., Xue, S., Hartley, W., Wu, H., 2016. Effects of iron-aluminium oxides and
669 organic carbon on aggregate stability of bauxite residues. Environ. Sci. Pollut. Res. 23, 9073-
670 9081.
671
672
673
674
675
676
677
678
679
680
681
682
683
684
685
686
687
688
689
690
691
692

693 **Table 1** Phosphorus (P) adsorption studies that have been carried out using bauxite residues, untreated
694 and treated residues, and their recovery efficiencies.

	P recovery technique	Factors investigated	Type of water	Initial P concentration of the water	P recovered	Reference
Untreated bauxite residue	Batch adsorption experiment	Kinetics, pH and temperature	Synthetic water	5-100 mg P L^{-1}	0.20 mg P g^{-1}	Grace *et al.* 2015
Gypsum Treated	Batch adsorption experiment	Contact time (3, 6, 24, 48hr)	Synthetic water	20-400 mg P L^{-1}	7.03 mg P g^{-1}	Lopez *et al.* 1998
Brine treated bauxite residue (Bauxsol™*)	Batch adsorption experiment	pH, ionic strength, time	Synthetic water	0.5-2 mg P L^{-1}	6.5-14.9 mg P g^{-1}	Akhurst *et al.* 2006
Acid and brine treated bauxite residue (Bauxsol™*)	Batch adsorption experiment	Kinetics and isotherms	Synthetic water	200 mg P L^{-1}	55.72 mg P g^{-1}	Ye *et al.* 2014
Heat treated bauxite residue	Batch adsorption experiment	Time, pH and initial concentration	Synthetic water	155 mg P L^{-1}	155.2 mg P g^{-1}	Liu *et al.* 2007
Acid and heat treated bauxite residue	Batch adsorption experiment	Time, pH and initial concentration	Synthetic water	155 mg P L^{-1}	202.9 mg P g^{-1}	Liu *et al.* 2007
Acid treated bauxite residue	Batch adsorption experiment	Acid type, pH	Synthetic water	1 mg P L^{-1}	1.1 mg P g^{-1}	Huang *et al.* 2008

695 *Bauxsol™ = neutralised bauxite residue produced using the Basecon™ procedure, which uses brines high in
696 Ca^{2+} and Mg^{2+} (McConchie *et al.* 2001).
697
698
699
700
701
702
703
704
705

706 **Table 2** Mineralogical composition of the bauxite residues, untreated and treated.
707

Parameter	Untreated Fine (UF)	Fine +gypsum (UFG)	Fine+ seawater (UFS)	Untreated Coarse (UC)	Coarse+ gypsum (UCG)	Coarse +seawater (UCS)	Untreated French (UFR)	French+ gypsum (UFRG)	French +seawater (UFRS)
Fe_2O_3 (%)	43.9±1.1	40.6±0.6	41.8±1.2	64.0±5.1	61.4±3.0	69.9±3.8	43.9±0.6	47.9±0.5	53.3±5.8
Al_2O_3 (%)	12.7±0.6	11.3±1.0	11.1±2.5	19.4±1.8	11.1±0.6	7.4±0.7	14.0±1.0	11.2±0.3	11.4±2.2
CaO (%)	5.9±0.2	8.2±0.5	4.4±0.3	1.1±0.2	7.6±0.4	1.2±0.1	5.6±0.1	7.7±0.3	3.2±0.5
MgO (%)	3.6±1.3	3.5±0.8	3.1±1.0	4.7±1.8	3.6±0.8	2.6±0.6	4.1±0.6	3.8±0.9	3.2±1.6
SiO_2 (%)	8.6±0.7	8.5±0.9	8.6±1.7	2.6±0.3	1.3±0.2	1.4±0.2	9.4±0.5	5.1±0.4	4.3±0.3
TiO_2 (%)	2.4±0.3	2.1±0.6	2.7±0.1	0.9±0.1	1.0±0.1	2.1±0.6	2.5±0.02	2.3±0.1	2.3±0.5
P_2O_5 (%)	0.6±0.04	0.4±0.02	0.4±0.1	0.3±0.02	0.2±0.02	0.2±0.06	0.5±0.01	0.5±0.02	0.5±0.01

Table 3 Elemental composition of the bauxite residues, untreated and treated.

Parameter	Untreated Fine (UF)	Fine +gypsum (UFG)	Fine+ seawater (UFS)	Untreated Coarse (UC)	Coarse+ gypsum (UCG)	Coarse +seawater (UCS)	Untreated French (UFR)	French+ gypsum (UFRG)	French +seawater (UFRS)
B (mg kg^{-1})	470±8.81	425±29	448±13	615±13.3	622±29	722±32.1	566±18.9	539±25	483.8±31
Al (mg kg^{-1})	72538±1390	81095±1219	80608±3090	45854±2769	48851±2336	45917±2080	67295±3343	65389±1326	64189±595
As (mg kg^{-1})	21.9±1.73	9.7±0.4	<LOD[1]	<LOD[1]	<LOD[1]	<LOD[1]	8.1±0.2	9.75±0.6	6.51±0.43
Ba (mg kg^{-1})	43.8±1.19	29.4±5	33.3±0.7	13.9±1.01	18.3±3.4	12.7±2.8	45.7±1.5	41.4±1.4	49.4±3.8
Cd (mg kg^{-1})	8.033±0.16	7.02±0.3	7.33±0.19	10.7±0.18	10.8±0.5	11.8±0.59	9.31±0.2	8.87±0.3	8.21±0.3
Cr (mg kg^{-1})	1698±37.2	933±44	1170±12.9	880±3.8	817±13	803±21.3	1184±15.9	1090±9	1159±31.2
Fe (mg kg^{-1})	338571±3057	289459±18597	298282±4937	434739±9980	460078±23043	471204±25753	353392±10003	328114±4498	332251±3435
Pb (mg kg^{-1})	34.88±0.54	27.8±2.8	36.9±0.8	29.56±3.03	24.6±3	22.06±2.47	34.5±0.9	32.3±0.8	37.4±2.1
Mg (mg kg^{-1})	122.28±4.96	163±37	1047±25.6	18.32±4.78	8.5±2.21	511.6±25.4	109±3.9	150±9	2203.8±134
Mn(mg kg^{-1})	163±2.63	140±6.1	167±6.8	187±15.5	223±99	185±31.1	134±0.9	139±1.9	142.9±4.2
Ni (mg kg^{-1})	18.6±0.89	<LOD[1]	2.25±0.2	3.54±0.27	3.15±0.5	4.18±0.22	1.1±0.1	1.24±0.2	1.23±0.3
K (mg kg^{-1})	391±13.68	454±29	1108±41	255±38	195±23	556.99±67.38	399±13	359±11	1048±63.2
Si (mg kg^{-1})	223.5±46.1	256±92	245.7±35	213±6.6	234±34	194.46±10.58	276±20	285±34	258.5±11.7
Na (mg kg^{-1})	28347±553	38180±352	41864±2012	8804±666	5935±114	11101.55±1121.8	25514±317	23703±499	31974±1087
Ti (mg kg^{-1})	1395±196	1309±100	1265±22	<LOD[1]	<LOD[1]	<LOD[1]	1382±38	1288±120	1233±46
V(mg kg^{-1})	1050±21.6	781±29	777±8	786±23.6	731±20	731.04±23	1036±12	920±7	983±21
Zn (mg kg^{-1})	50.7±0.71	40.6±1.2	42.6±1.3	86.7±1.7	82±5.4	84.68±4.2	55.8±0.5	55.6±1.17	57.3±0.9
Ga(mg kg^{-1})	78.9±2.02	81.2±0.53	73.9±0.6	71.8±1.03	69.3±2.3	73.5±1.6	86.8±1.3	78.6±2	78.8±0.9
Ca(mg kg^{-1})	46657±832	51641±485	17159±413	4152±490	12771±823	4089.42±588.32	15084±358	42703±2383	14820±926
P(mg kg^{-1})	955±0.57	962±99	1018±15	1040±23	1011±59	1039.6±23	1298±26	1220±10	1320±53.8
Be(mg kg^{-1})	<LOD[1]	<LOD[1]	<LOD[1]	<LOD[1]	<LOD[1]	<LOD[1]	<LOD[1]	<LOD[1]	<LOD[1]
Cu (mg kg^{-1})	<LOD[1]	<LOD[1]	<LOD[1]	<LOD[1]	<LOD[1]	<LOD[1]	<LOD[1]	<LOD[1]	<LOD[1]
Hg (mg kg^{-1})	<LOD[1]	<LOD[1]	<LOD[1]	<LOD[1]	<LOD[1]	<LOD[1]	<LOD[1]	<LOD[1]	<LOD[1]
Mo(mg kg^{-1})	<LOD[1]	<LOD[1]	<LOD[1]	<LOD[1]	<LOD[1]	<LOD[1]	<LOD[1]	<LOD[1]	<LOD[1]
Se (mg kg^{-1})	<LOD[1]	<LOD[1]	<LOD[1]	<LOD[1]	<LOD[1]	<LOD[1]	<LOD[1]	<LOD[1]	<LOD[1]

708 [1]<LOD = below the limits of detection.

709 **Table 4** Physical and chemical characterisation of the bauxite residues, untreated and treated.
710

Parameter	Untreated Fine (UF)	Fine +gypsum (UFG)	Fine+ seawater (UFS)	Untreated Coarse (UC)	Coarse+ gypsum (UCG)	Coarse +seawater (UCS)	Untreated French (UFR)	French+ gypsum (UFRG)	French +seawater (UFRS)
pH	10.8±0.12	8.7±0.04	9.02±0.07	11.4±0.29	6.79±0.08	7.95±0.16	11.9±0.06	9.17±0.02	9.49±0.01
EC (µS cm^{-1})	704±90.8	1338±3.5	3080±17.3	856±1.53	909±2	916±1.53	1184±48.8	1219±7.21	5323±172
% Water	23.5±0.65	28.9±0.6	32.1±1.72	0.39±0.2	0.82±0.18	3.13±0.72	28±0.54	35.3±1.32	36.5±0.16
d_{10} (µm)[a]	0.6±0.09	1.37±0.23	1.26±0.06	1.27±0.47	1.11±0.23	1.66±0.83	1.3±0.04	1.49±0.06	1.08±0.74
d_{50} (µm)[b]	2.43±0.29	3.56±0.59	3.52±0.11	5.13±0.63	3.69±0.49	3.68±0.4	3.7±0.12	4.11±0.39	3.47±0.98
d_{90} (µm)[c]	6.02±0.86	7.12±1.98	7.69±1.97	12.04±1.27	9.51±0.25	7.0±0.13	10.11±2.37	9.81±2.68	7.17±3.25
Total Pore Space (%)[d]	50.03±2.25	50.73±9.04	50.03±1.75	9.63±6.46	10.82±1.09	7.65±5.26	61.77±1.16	53.6±1.95	53.87±0.78
Bulk Density (g cm^{-3})[e]	1.5±0.02	1.5±0.01	1.49±0.01	2.53±0.01	2.48±0.03	2.55±0.01	1.31±0.03	1.32±0.03	1.31±0.02
Particle Size Density (g cm^{-3})[f]	2.99±0.1	3.11±0.5	2.94±0.12	2.81±0.21	2.65±0.4	2.7±0.14	3.41±0.07	2.85±0.08	2.85±0.07
PZCpH[g]	6.96±1.21	3.43±0.73	6.28±0.98	6.89±0.09	3.11±0.12	6.39±0.51	6.16±0.21	6.32±0.51	4.43±0.09
CEC (K)(cmol kg^{-1})[h]	63.3±2.56	64.1±3.41	60.1±2.96	N/A[k]	N/A[k]	N/A[k]	57.5±2.13	56.4±3.49	48.9±13.7
Total Pore Volume (cm^{-3} g^{-1})[i]	0.03	0.03	0.03	0.02	0.02	0.03	0.03	0.04	0.03
BET SSA (m^2 g^{-1})[j]	11.73	12.77	13.82	12.58	13.19	15.37	15.24	17.57	17.57

711 [a]d_{10} (µm) = the size of particles at 10% of the total particle distribution, expressed in µm.
712 [b]d_{50} (µm) = the median; the size of particles at 50% of the total particle distribution, expressed in µm.
713 [c]d_{90} (µm) = the size of particles at 90% of the total particle distribution, expressed in µm.
714 [d]Total Pore Space = the total pore space which may be calculated from particle density and bulk density.
715 [e]Bulk density = the mass of soil per unit volume, expressed as g cm^{-3}.
716 [f]Particle size density = the density of the solid particles, excluding pore spaces between them, expressed as g cm^{-3}.
717 [g]PZCpH = the pH at which the point of zero charge is occurring.
718 [h]CEC= the cation exchange capacity, expressed as cmol kg^{-1}.
719 [i]BET SSA = specific surface area analysed using Brunauer-Emmett-Teller isotherm and expressed as m^2 g^{-1}.
720 [j]Total Pore Volume = measurement of total pore volume expressed as cm^{-3} g^{-1}.
721 [k]N/A =not available

Table 5 Maximum adsorbency (mg P g^{-1} media) of P using each of the bauxite residue samples, untreated and treated (level of fit of the data, R^2, to Langmuir isotherm is included in brackets).

Media	Treatment method employed		
	Untreated	Gypsum	Seawater
	---------- mg P g^{-1} media ----------		
UFR	1 (0.99)	2.73 (0.99)	1.92 (0.99)
UF	0.38 (0.99)	2.46 (0.97)	0.48 (0.99)
UC	0.35(0.98)	1.39 (0.99)	0.66 (0.99)

UF

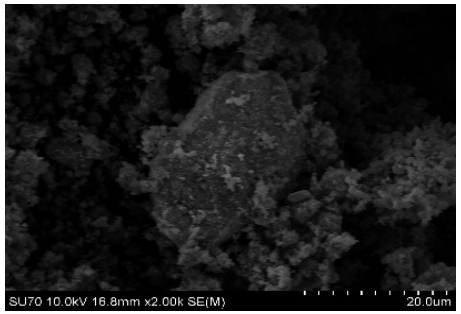

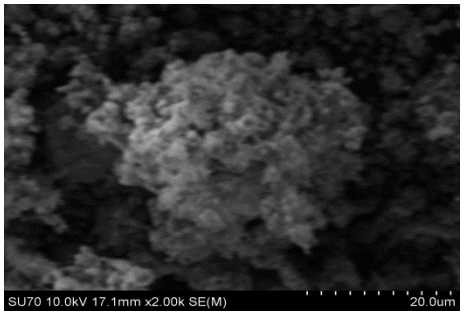

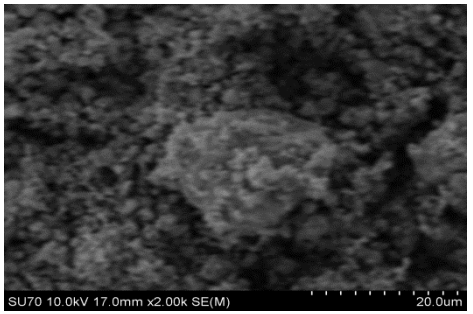

UC

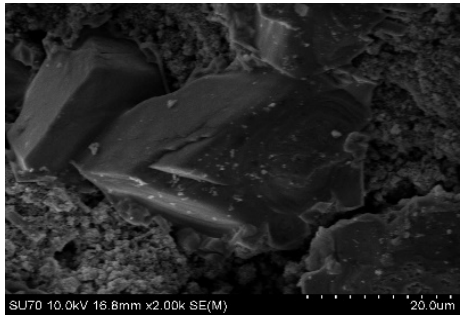

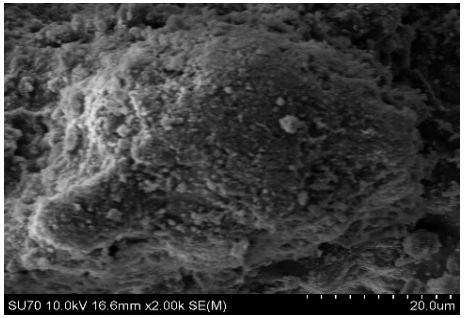

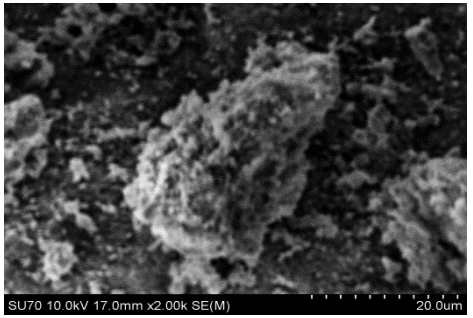

UFR

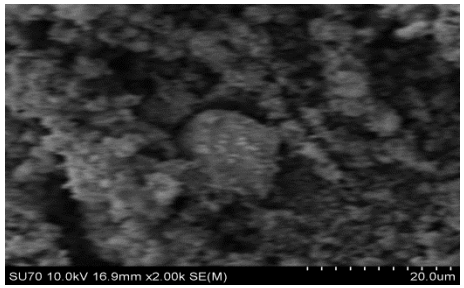

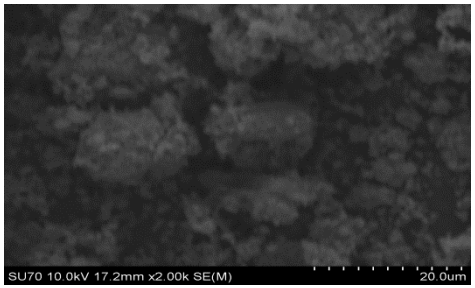

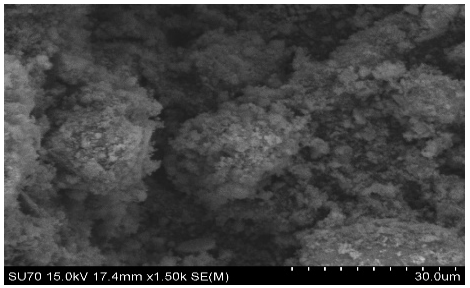

Untreated **Gypsum Treated** **Seawater Treated**

Figure 1. SEM (10kV; magnification x2,000; working distance 16.8mm) imaging for the three untreated bauxite residue pre and post treatment with either gypsum or seawater.

741